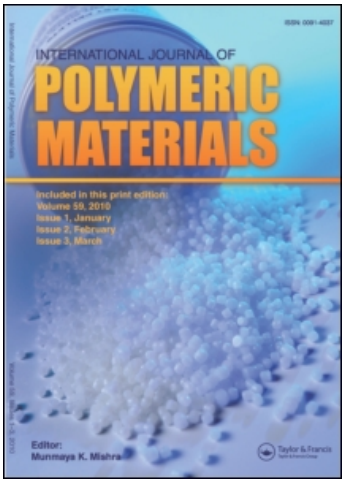

International Journal of Polymeric Materials
Publication details, including instructions for authors and subscription information:
http://www.informaworld.com/smpp/title~content=t713647664

Changes in the Amorphous Phase of Polyethylene upon High Extension

G. K. Elyashevich[a]; E. A. Karpov[a]; V. K. Lavrentiev[a]; V. I. Poddubny[b]; M. A. Genina[c]; Yu. F. Zabashta[c]
[a] Institute of Macromolecular Compounds, Russian Academy of Sciences, St. Petersburg, Russia [b] A. I. Herzen Russian State Pedagogical University, St. Petersburg, Russia [c] Physical Department, T. G. Shevchenko State University, Kiev, Ukraina

To cite this Article Elyashevich, G. K. , Karpov, E. A. , Lavrentiev, V. K. , Poddubny, V. I. , Genina, M. A. and Zabashta, Yu. F.(1993) 'Changes in the Amorphous Phase of Polyethylene upon High Extension', International Journal of Polymeric Materials, 22: 1, 191 — 199
To link to this Article: DOI: 10.1080/00914039308012074
URL: http://dx.doi.org/10.1080/00914039308012074

Intern. J. Polymeric Mater., 1993, Vol. 22, pp. 191–199
Reprints available directly from the publisher
Photocopying permitted by license only

Printed in Malaysia

Changes in the Amorphous Phase of Polyethylene upon High Extension

G. K. ELYASHEVICH, E. A. KARPOV, and V. K. LAVRENTIEV

Institute of Macromolecular Compounds, Russian Academy of Sciences, 31 Bol'shoi pr., St. Petersburg 199400, Russia

and

V. I. PODDUBNY

A. I. Herzen Russian State Pedagogical University, 38 Moika, St. Petersburg 199065, Russia

and

M. A. GENINA, and Yu. F. ZABASHTA

Physical Department, T. G. Shevchenko State University, Glushkova 6, Kiev 252127, Ukraina

The structure of noncrystalline regions of HDPE oriented filaments prepared by two different techniques with various degrees of orientation λ has been studied by density measurements, small-angle X-ray scattering and DTA. It is shown that at $\lambda > 10$ the noncrystalline regions of the oriented structure prepared from a crystallized material have 80 nm voids (pores) in addition to an amorphous phase. The volume fraction of pores grows with increasing λ. If a sample is prepared by crystallization from a pre-oriented melt, it does not contain discontinuities, and its noncrystalline regions consist of the amorphous material alone. In this case the density of the amorphous phase does not depend on the degree of sample orientation and has a constant magnitude typical of highly oriented PE samples.

KEY WORDS Polyethylene, uniaxial drawing, orientational crystallization, high strength, high modulus, pores.

INTRODUCTION

It is established that two competing processes occur simultaneously during uniaxial drawing of a crystallized flexible-chain polymer, i.e. strengthening resulting from unfolding and parallel arrangement of macromolecules along the draw axis and fracture caused by rupture of stressed tie chains and splitting of crystallites. At low draw ratios λ, strengthening dominates, at high λ fracture begins to play an ever increasing role and limits further enhancement of mechanical characteristics.[1,2] Our studies have shown that at high λ, close

to the ultimately attainable ones, fracture gives rise to irreversible changes in the sample that strongly affect the behavior of mechanical characteristics (tensile strength and modules of elasticity) with λ.

This work was aimed at a study of changes occurring in the noncrystalline part of a sample during the preparation of highly oriented PE films and filaments. The samples were prepared from an extruded melt by two techniques: (i) crystallization initiated by a preliminary melt extension (orientational crystallization)[3–5] and (ii) uniaxial drawing of a crystallized initial structure (orientational drawing).[1,2,6] Densities of the samples obtained by both techniques were measured, and densities of noncrystalline regions as functions of draw ratio were estimated. Moreover, X-ray scattering was used to study the density distribution to reveal the presence of inhomogeneities in these regions. To estimate the density of noncrystalline regions, the degree of crystallinity was calculated from the DTA measurements of the melting enthalpy of the samples.

EXPERIMENTAL

Films and filaments of commercial HDPE with $M_w = 235\,000$ and $M_w/M_n = 6$–8 were studied. In preparation of films by orientational crystallization, the extruded melt entered the heating drum cooled to a temperature close to the melting temperature and stretched thereafter so that crystallization and solidification occurred in the extension zone of the filament.[3–6] In orientational drawing, the extruded melt entered a quenching bath with water at 10°C immediately after it left the spinneret. In the bath it rapidly crystallized, and the solidified film was subjected to uniaxial drawing at 110°C to a desired draw ratio λ. Some samples were subjected to a second stage of drawing[6] at 115°C. In both processes, transition into the oriented state occurred forming a "neck".

Densities of the oriented samples ρ were determined by hydrostatic weighing and were calculated from $\rho = \rho_l m/(m-m_l)$, where m and m_l were the weights counterbalancing the sample in the air and liquid, respectively, ρ_l is the density of the liquid (a mixture of water and spirit), ρ_l being measured by an areometer.

Small-angle X-ray measurements were performed by a Kratky camera. A CuK_α radiation filtered by a Ni-filter was used. To obtain the whole scattering curve an input and output slits 100 μm and 250 μm in size, respectively, were used. The initial portion of the scattering curve needed to define the Guinier radius was obtained with 10 μm and 20 μm slits.

A specific melting enthalpy ΔH was found from the DTA curves obtained by a Paulik–Erden Q-1500 derivatograph (Hungary).

Using the DTA data, the mass degree of crystallinity was calculated from

$$\alpha = \frac{\Delta H}{\Delta H_0}, \tag{1}$$

where ΔH_0, a specific melting enthalpy of an ideal crystal, was taken to be 293 kJ kg^{-1} for PE.[7]

CALCULATION OF DENSITY OF NONCRYSTALLINE REGIONS

The density of noncrystalline regions ρ' was calculated using the following assumptions.

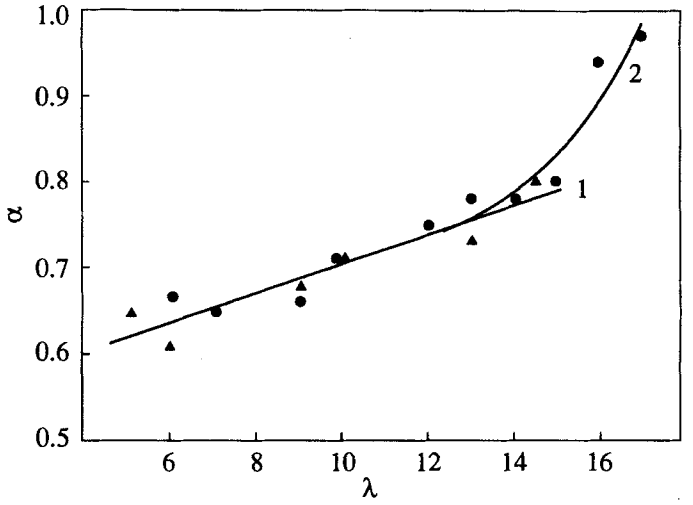

FIGURE 1 Mass degree of crystallinity as a function of draw ratio λ for samples prepared by orientational crystallization (▲, curve 1) and orientational drawing (●, curve 2).

A sample volume V was taken to be the sum of the crystalline V_c and noncrystalline V' regions: $V = V_c + V'$. Hence $M/\rho = M_c/\rho_c + M'/\rho'$, where M is the sample mass, M' is the mass of noncrystalline part of the sample, and ρ_c, i.e. density of crystalline regions, was taken[8] to be 1000 kg m^{-3}.

We rewrite the previous expression as:

$$\frac{1}{\rho} = \frac{M_c}{M}\frac{1}{\rho_c} + \frac{M'}{M}\frac{1}{\rho'}.$$

Since $M_c/M = \alpha$ and $M'/M = 1 - \alpha$, the density of noncrystalline regions can be given by

$$\rho' = \frac{(1-\alpha)\rho\rho_c}{\rho_c - \alpha\rho}. \tag{2}$$

By finding experimentally ρ and ΔH for a sample with a given λ and thereby calculating its α and ρ' from expressions (1) and (2), respectively, we can determine α, ρ, and ρ' as functions of λ for the samples prepared by the techniques described above.

Note that if the sample is amorphous-crystalline and has no voids, its ρ' will be equal to the density of the amorphous region ρ_a. In the opposite case, i.e. when the sample has voids, these values will be different.

RESULTS AND DISCUSSION

Densities of the samples ρ and their mass degrees of crystallinity α were measured as functions of draw ratio λ that was defined as a degree of melt extension before its crystallization in technique (i) and as a draw ratio of a crystallized sample in technique (ii). The experimental curves show that both the mass degree of crystallinity α (Figure 1) and density ρ (Figure 2) grow with increasing λ for the samples prepared by both techniques; however

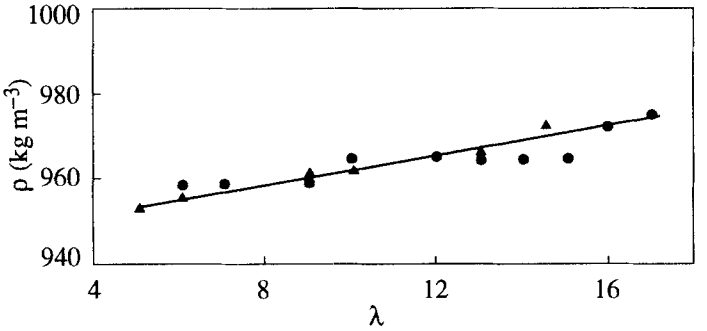

FIGURE 2 Density ρ as a function of draw ratio λ for samples prepared by orientational crystallization (▲) and orientational drawing (●).

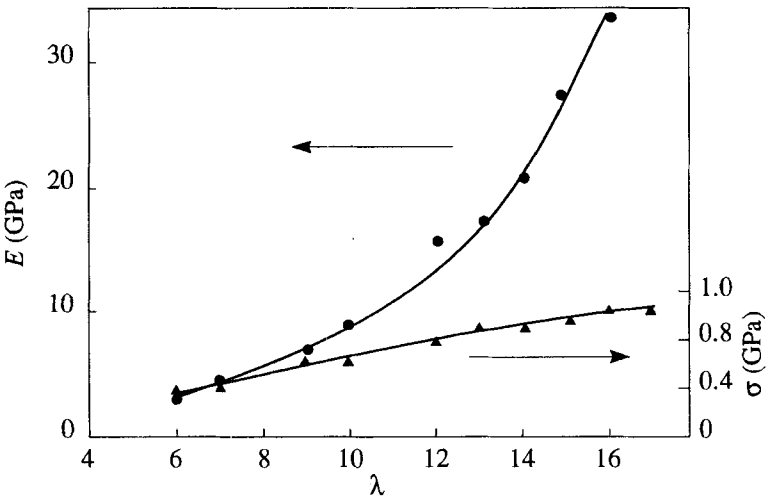

FIGURE 3 Modules of elasticity E and tensile strength σ versus draw ratio λ for PE filaments prepared by orientational drawing.

the behavior of these curves is different, i.e. the samples of the second type exhibit a steeper growth of α with λ at $\lambda > 10$ as compared to the initial linear portion. The mechanical characteristics, i.e. tensile strength σ and modules of elasticity E, were measured for all samples. They were also found[6] to grow with λ (Figure 3). However, the dependences of densities of noncrystalline regions ρ' on λ behave in different fashions for the samples prepared by techniques (i) and (ii) (Figure 4). In an orientationally crystalized material ρ' remains unaffected over the whole range of variations of λ and has the magnitude typical of the amorphous phase density in oriented PE samples.[7,8] For uniaxially stretched samples ρ' equals that of the (i)-samples at $\lambda < 10$, then it begins to decrease with increasing λ and even falls below the density of the amorphous phase of unoriented PE[7,8] that equals approximately 850 kg m^{-3}.

To explain this unexpected fact, the X-ray studies of samples obtained by one- and two-stage drawing were carried out. The small-angle X-ray pattern for the samples with low $\lambda(\lambda < 10)$ exhibits one peak that corresponds to a long period $L_1 = 24$ nm (Figure 5,

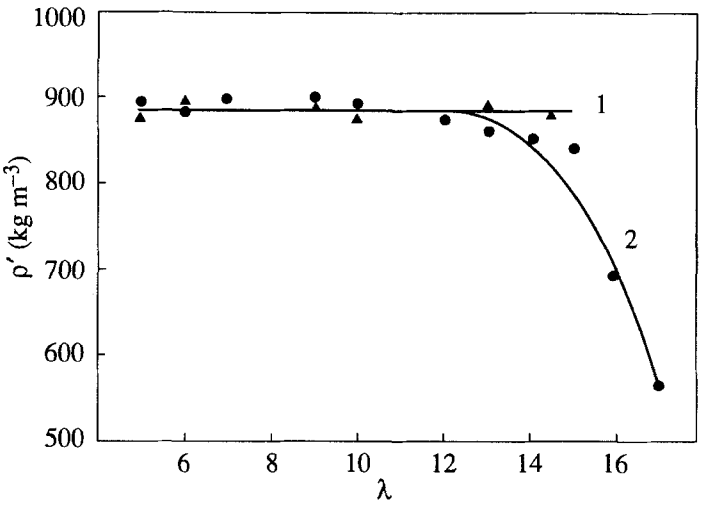

FIGURE 4 Density of noncrystalline regions ρ' as a function of draw ratio λ for samples prepared by orientational crystallization (▲, curve 1) and orientational drawing (●, curve 2).

curve 1) and characterizes a lamellar structure of the sample. At $\lambda = 11$ this peak has a "shoulder" (Figure 5, curve 2) that corresponds to the peak of scattering from the structure with a long period $L_2 = 30$ nm. The intensity deviations from the basic curve at this peak lie within 3% which nearly equals the instrumental error. However, the scattering curves are fully reproducible (10 scans were made for each λ). This fact makes the results sufficiently reliable. Moreover, this maximum is observed only for the samples with $\lambda = 10$–16 and its angular position remains the same. When λ grows the intensity of this peak somewhat increases in comparison with the intensity of the first peak (Figure 5, curve 3). The intensity of the second peak is from one sixth to one tenth of the intensity of the first peak. However, it increases with increasing λ at the first stage of drawing, and the intensity of the first peak decreases (Figure 5, curve 3). These changes in the X-ray pattern that are accompanied by a considerable growth of strength σ and modules of elasticity E of the sample (Figure 3) are caused by formation and growth of fibrillar structures containing extended chains during drawing. A difference between the densities of crystalline and amorphous regions in these fibrils is much smaller than in the lamellar structures because of thickening of the amorphous material during drawing. This explains a lower intensity of scattering from them.

Disappearance of the shoulder at the second stage of drawing that takes place at a temperature higher than that at the first stage is likely to be due to an increase of the fraction of straightened and extended chains in the amorphous regions of fibrils. As a consequence, densities of the crystalline and amorphous regions become equal, and discrete small-angle scattering from the fibrillar structure in the samples prepared by two-stage drawing disappears (Figure 5, curve 4).

In addition to discrete scattering, the X-ray patterns of the samples obtained by orientational drawing also display diffuse scattering that is observed at all λ. For the quantitative analysis, the initial portion of the diffuse scattering curve was used. The curve was obtained for the scattering angles ranging from 1.5′ to 10′ using the entrance and the exit slits 10

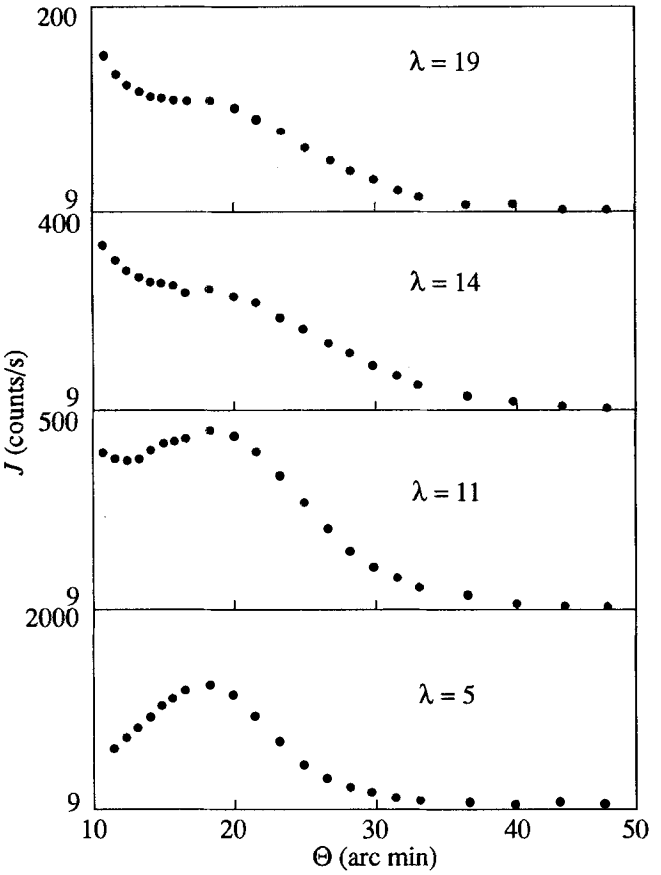

FIGURE 5 Angular dependencies of small-angle X-ray scattering intensity for PE filaments prepared by orientational drawing with various λ.

and 20 microns in size, respectively (Figure 6). This scattering is caused by the presence of scattering elements, most likely voids, whose size, as shown by the Guinier analysis of scattering curves, is 60 nm at $\lambda = 5$. The Guinier analysis shows that the sizes of these pores in the direction of drawing and in the perpendicular direction are similar. This proves that the shape of these pores is nearly spherical. As λ grows their shape transforms into an elliptical one, i.e. the size of the ellipsoid along the draw axis increases up to 800 Å and the transverse size remains unaltered (Figure 6). Scanning from the inhomogeneities smaller in size than those mentioned above does not appreciably affect the calculation results. The number of pores increases steadily, which is indicated by a growth of diffuse scattering intensity. A comparison of the size of these pores with the long period leads to a conclusion that they are localized in the interfibrillar space, and it is these pores that can provide a free volume needed for transition from the lamellar to the fibrillar structure. The appearance of the shoulder on the small-angle X-ray pattern, which is the evidence of the onset of this transition, takes place at the λ when the pore size is the largest (~ 80 nm).

Thus, reduction in the X-ray scattering intensity with increasing λ for the samples obtained by technique (ii) results from a decreasing difference between the densities of

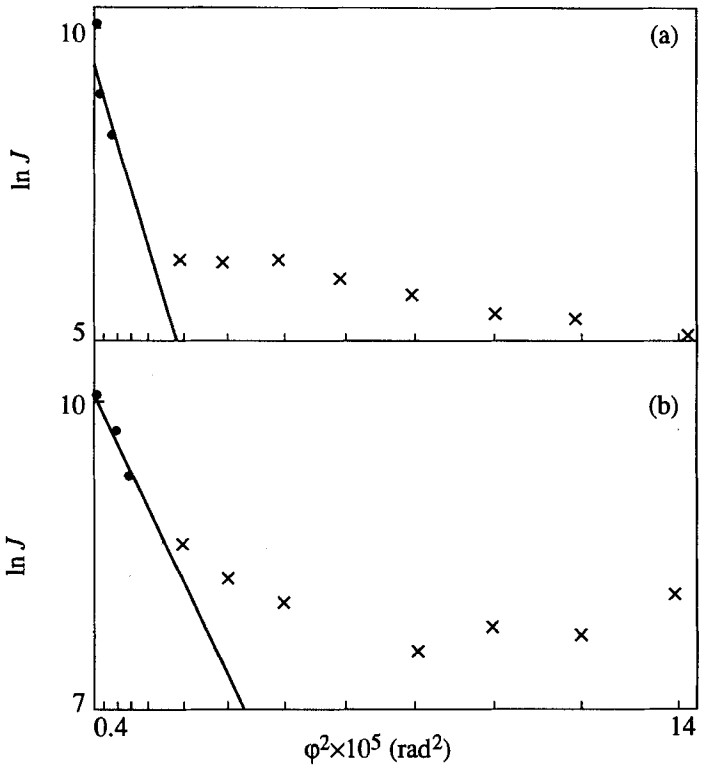

FIGURE 6 The Guinier-plot for the sample with $\lambda = 12$ in (a) the direction of drawing and (b) the perpendicular direction.

crystalline and amorphous regions, i.e. an increasing density of amorphous regions within fibrils ρ_a. As noted above, the density of noncrystalline regions in the sample ρ' drops in this case. This fall and a simultaneous increases of ρ_a indicate that the regions of much lower density, i.e. voids, appear in the noncrystalline part. The presence of these voids is confirmed by intense diffuse scattering.

Let us estimate the fraction of these voids. The volume of the noncrystalline part of the sample V' is the sum of the volume of the amorphous phase V_a and volume of pores V_0:

$$V' = V_a + V_0. \tag{3}$$

The total volume V of the sample is then given by

$$V = V_c + V_a + V_0. \tag{4}$$

By denoting the fraction of pores in the total volume of the sample by $X = V_0/V$, we get

$$X = 1 - \frac{V_a}{V} - \frac{V_c}{V}. \tag{5}$$

The volumes of the crystalline and amorphous phases are expressed through corresponding masses and densities as $V_a = M_a/\rho_a = (1 - \alpha)M/\rho_a$ and $V_c = M_c/\rho_c = \alpha M/\rho_c$,

where M_a is mass of the amorphous part of the sample. Then

$$X = 1 - \rho\left(\frac{\alpha}{\rho_c} + \frac{1-\alpha}{\rho_a}\right). \tag{6}$$

The fraction of pores in the noncrystalline part is given by $X' = V_0/V'$. By expressing V_0 from Equation (3), we obtain $X' = 1 - V_a/V'$ and, since $V' = M_a/\rho'$, $X = 1 - \rho'/\rho_a$.

Since at $\lambda < 10$ the samples prepared by drawing exhibit a constant ρ' equal to a typical density of amorphous regions in oriented PE samples (compare curves 1 and 2 in Figure 2), and a drastic decrease of ρ' begins at $\lambda > 10$ (Figure 4), we assumed that at $\lambda < 10$ $\rho' = \rho_a = 890$ kg m^{-3} (see Figure 2) and a further fall of ρ' is caused by formation of pores, while the density of amorphous regions themselves ρ_a remains unaltered.

On these assumptions, X' and X calculated from Equations (6) and (7) were found to be 30% and 2%, respectively, at $\lambda = 17$. Note that these magnitudes of X' and X are underestimated, because in practice ρ_a is not constant, as was assumed, but grows with λ at fairly high draw ratios. However, we did not allow for these changes of ρ_a, since this growth is difficult to estimate qualitatively from the experimental data.

Note that the formation of these pores does not affect the mechanical characteristics of a sample, because these voids are located in the interfibrillar regions that do not bear mechanical loads. Their formation is a result of the structural "need" for a free volume at the stage of rearrangement inside the fibrils that gives rise to unfolding of macromolecules initially folded in crystals, which leads to strengthening and eventual thickening of the material.

At the second stage of drawing, the amount of voids with the size indicated above decreases sharply (diffuse scattering almost disappears) due to a transverse compression of the sample at high λ. At this stage, however, (at $\lambda > 16$) discontinuities lying in the direction normal to the orientation direction appear in the sample. They are well seen through an optical microscope (Figure 7) and cause visual whitening of the sample at ultimate λ, close to the breakdown ones. Formation of these cracks is likely to be initiated by kink bands earlier observed in ultimately oriented PE samples.[9] These cracks are traversed by extended tie chains aligned along the orientational direction and bearing loads during sample drawing. The tie chains that consist of a highly oriented material are the structural elements responsible for high strength and elastic characteristics of the sample. However, strength no longer grows with further increase of λ at the second stage of drawing, since the cracks are formed due to the development of fracture processes.

It is important to note that orientationally crystallized samples do not contain pores at any λ, which is due to the formation of their crystalline structure directly from the oriented melt, while formation of highly oriented structures on drawing results from the transformation of an initial lamellar structure into a fibrillar one under orienting mechanical stresses. It is due to the fact that in the melt molecules are distributed uniformly, and molecular interactions are symmetric with respect to the neighboring molecules and depend on the distance alone between them. In case of a crystallized solidified system this symmetry is disturbed, because there is a much stronger interaction between the molecules in a crystallite than between crystallites themselves. Therefore, when such a structure is deformed, parts of a material are pulled out by stressed molecules nonuniformly and are

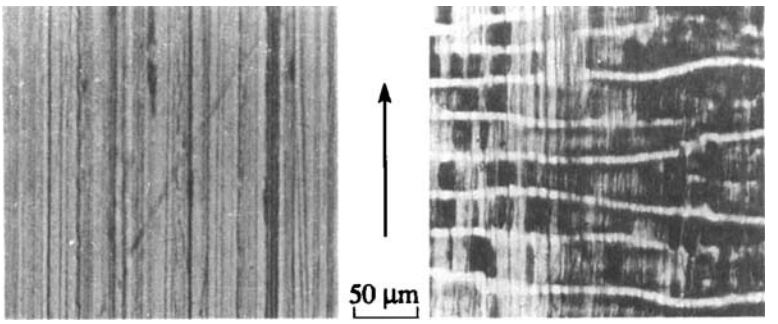

FIGURE 7 Optical microphotographs of PE films prepared by orientational crystallization (left) and of filaments prepared by orientational drawing (right). Arrows show orientation direction.

displaced relatively to each other in blocks, which requires the formation of a sufficiently large free volume that cannot easily leave the sample as in the melt and remains in the form of pores after deformation. On melt orientation, a high mobility of macromolecules and the absence of ordered structural elements provide extension of a viscous material without micropore formation, and crystallization of an oriented melt results in the formation of a system that does not contain pores and other discontinuities.

CONCLUSION

The disordered regions of highly oriented PE samples produced by two considered techniques has been found to have a different structure. In contrast to the orientationally crystallized films, the samples produced by drawing contain micropores, the latter being formed in the initial stage of drawing. Further drawing leads to the development of the other type pores whose long axes are oriented perpendicular to the drawing direction. Their appearance is accompanied by the whitening of drawn films or fibers and hinders the growth of tensile strength with drawing. The additional drawing of orientationally crystallized samples does not results in the initiation of pores in a whole range of draw ratios achieved. The elastic modulus of orientationally crystallized samples grows with drawing but their tensile strength, however, almost does not change.

References

1. V. A. Marikhin and L. P. Myasnikova, *Supermolecular Structure of Polymers*, (Khimiya, Leningrad, 1977) (in Russian).
2. L. P. Myasnikova, *Plaste und Kautschuk*, **33**, 4, 121 (1986).
3. V. G. Baranov, *Khim. Volokna*, **3**, 14 (1977) (in Russian).
4. G. K. Elyashevich, V. G. Baranov, and S. Ya. Frenkel, *J. Macromol. Sci. Phys.*, **B13**, 255 (1977).
5. G. K. Elyashevich, *Adv. Pol. Sci.*, **43**, 205 (1982).
6. G. K. Elyashevich, B. V. Streltses, E. A. Karpov, V. A. Marikhin, L. P. Myasnikova, E. A. Ro, and E. Yu. Rozova, *5th Inter. Symp. on Man-Made Fibers*, (Kalinin, 1990), Vol. 2, p. 127.
7. L. Mandelkern, *Crystallization of Polymers*, (McGraw-Hill, New York, 1964).
8. D. V. van Krevelen, *Properties of Polymers: Their Estimation and Correlation with Chemical Structure*, (Elsevier, Amsterdam-London-New York, 1972).
9. E. A. Egorov, V. V. Zhizhenkov, V. A. Marikhin, and L. P. Myasnikova, *J. Macromol. Sci. Phys.*, **B29**, 2–3, 249 (1990).